NIH Public Access
Author Manuscript
J Immunol. Author manuscript; available in PMC 2010 July 1.

Published in final edited form as:
J Immunol. 2009 July 1; 183(1): 661–669. doi:10.4049/jimmunol.0900274.

Macrophage delivery of nanoformulated antiretroviral drug to the brain in a murine model of neuroAIDS[1]

Huanyu Dou[*], **Cassi B Grotepas**[*], **JoEllyn M McMillan**[*], **Christopher J. Destache**[†], **Mahesh Chaubal**[‡], **Jane Werling**[‡], **James Kipp**[‡], **Barrett Rabinow**[‡], and **Howard E. Gendelman**[*,‖,2]

[*]Department of Pharmacology and Experimental Neuroscience, Omaha, NE 68198

[‖]Department of Internal Medicine University of Nebraska Medical Center, Omaha, NE 68198

[†]School of Pharmacy and Health Professions Creighton University, Omaha, NE 68178

[‡]Baxter Healthcare Corporation, Round Lake, IL 60073

Abstract

Antiretroviral therapy (ART) shows variable blood-brain barrier penetration. This may affect the development of neurological complications of human immunodeficiency virus (HIV) infection. In attempts to attenuate viral growth for the nervous system, cell-based nanformulations were developed with the focus on improving drug pharmacokinetics. We reasoned that ART carriage could be facilitated within blood-borne macrophages traveling across the blood-brain barrier. To test this idea, an HIV-1 encephalitis (HIVE) rodent model was employed where HIV-1-infected human monocyte-derived macrophages were stereotactically injected into the subcortex of severe combined immunodeficient mice. ART was prepared using indinavir (IDV) nanoparticles (NP, nanoART) loaded into murine bone marrow macrophages (BMM, IDV-NP-BMM) after *ex vivo* cultivation. IDV-NP-BMM was administered intravenously to mice resulting in continuous IDV release for 14 days. Rhodamine-labeled IDV-NP was readily observed in areas of HIVE and specifically in brain subregions with active astrogliosis, microgliosis and neuronal loss. IDV-NP-BMM treatment led to robust IDV levels and reduced HIV-1 replication in HIVE brain regions. We conclude that nanoART targeting to diseased brain through macrophage carriage is possible and can be considered in developmental therapeutics for HIV-associated neurological disease.

Keywords

Monocytes/Macrophages; Neuroimmunology; Rodent; AIDS; Cell Trafficking

[1]This work was supported by grants 2R01 NS034239, 2R37 NS36126, P01 NS31492, P20RR 15635, P01MH64570, and P01 NS43985 (to H.E.G.) from the National Institutes of Health.

2Address correspondence to: Howard E. Gendelman, Department of Pharmacology and Experimental Neuroscience, University of Nebraska Medical Center, 985880 Nebraska Medical, Center, Omaha, NE 68198-5880; Phone: 402 559 8920; FAX: 402 559 3744; hegendel@unmc.edu.

Publisher's Disclaimer: This is an author-produced version of a manuscript accepted for publication in *The Journal of Immunology (The JI)*. The American Association of Immunologists, Inc. (AAI), publisher of *The JI*, holds the copyright to this manuscript. This version of the manuscript has not yet been copyedited or subjected to editorial proofreading by *The JI*; hence, it may differ from the final version published in *The JI* (online and in print). AAI (*The JI*) is not liable for errors or omissions in this author-produced version of the manuscript or in any version derived from it by the U.S. National Institutes of Health or any other third party. The final, citable version of record can be found at http://www.jimmunol.org.

Disclosures

The authors have no financial conflict of interest.

NIH-PA Author Manuscript
NIH-PA Author Manuscript
NIH-PA Author Manuscript

NIH-PA Author Manuscript

NIH-PA Author Manuscript

NIH-PA Author Manuscript

Introduction

In its most significant form, human immunodeficiency virus (HIV) associated neurocognitive disorders (HAND) are defined as cognitive, motor, and/or behavioral impairments. These are linked to progressive viral infection and immune deterioration (1). A substantive pathogenic event for disease is the infiltration of blood borne mononuclear phagocytes (MP: monocytes, tissue macrophages and microglia) into affected brain tissue. This accelerates viral dissemination in brain precipitating productive HIV replication and the subsequent formation of macrophage-derived multinucleated giant cells (MGC) (2–4). We reasoned that as the vehicle for virus carriage into the nervous system, MP could also be harnessed as an antiretroviral drug carrier (5,6). In this way, drug-loaded blood-borne macrophages would cross the blood-brain barrier (BBB) into diseased brain subregions and release antiretroviral drugs serving to improve its efficacy. The importance of this strategy is bolstered by antiretroviral therapy (ART) is known to reduce HAND severity. Indeed, HIV patients on ART live longer and neurological dysfunctions are reduced, showing a mixture of more mild disease with reduced viral replication (7–11). All together, improving ART BBB penetration could positively affect disease outcomes and as such, be an integral part of HIV treatments targeting the nervous system (8,12,13,14,15).

Current ART limitations are due to its inabilities to combat viral mutation and achieve continuous, effective drug levels in virus target tissues (12,16–18). Indeed, resistance to antiretroviral compounds can and often does develop; and when present HIV-1 levels can rapidly rebound to pretreatment concentrations if ART is discontinued (19–22). Such effects might be attenuated if optimal ART transport across tissue barriers could be achieved. One impediment in reaching this goal is the BBB. This tissue barrier serves to restrict macromolecular drug transport and as such effective drug concentrations (23–26).

A means to facilitate ART passage through the BBB is by using circulating monocyte-derived macrophages (MDM) as drug depots. Previously, our laboratory used laboratory and animal systems to pursue this idea. The research demonstrated that macrophages can deliver drug to sites of viral infection and show sustained antiretroviral activities (5,27). Recently, we also showed that bone marrow macrophages (BMM) can cross the BBB into HIV-1 infected brain regions (6). Based on these findings, a BMM pharmacologic nanoparticles (NP) delivery system (nanoART) was developed to test whether blood-borne macrophages could deliver ART directly to the brain. Our results demonstrate that BMM can serve as vehicles for indinavir (IDV) NP delivery. BMM showed consistent uptake and release of IDV-NP and free IDV while targeting areas of viral replication in a severe combined immunodeficient (SCID) model of HIV-1 encephalitis (HIVE). These data support the notion that nanoART brain penetration, drug distribution and therapeutic responses can be achieved through cell-based nanoformulation and as such lower drug-dosing intervals, adherence and bioavailability.

Materials and Methods

NP preparation and characterization

IDV-NP suspensions were prepared using high-pressure homogenization. The surfactant coating of the IDV crystals was made with 1.2% (w/v) Lipoid E80, an egg phosphatide mixture of phosphatidylcholine, phosphatidylethanoloamine, and the hydrolyzed lyso-forms (single aliphatic chain) of each phospholipid. Lipoid E80 coated the actual particles. The nanosuspension was made at an alkaline pH of 8.5. IDV free-base (1.2 g) was added to the phospholipid dispersion, and a pre-suspension manufactured using an Ultraturrax rotor-stator mixer for 4 minutes was used to reduce the particle size. An isotonic buffer solution was prepared by dissolving 1.8 g sodium chloride and 0.28 g sodium phosphate dibasic in 200 mL of water. The pre-suspension was homogenized at 15,000 psi for 40 passes. The final mean

NIH-PA Author Manuscript

NIH-PA Author Manuscript

NIH-PA Author Manuscript

NP size of the suspension was 1.6 μm, with 99% of the particles < 8.4 μm. The process was optimized for temperature, pressure and homogenization cycles. Particle size was optimized to minimize dissolution before and during macrophage uptake and measured using light scattering and suspension stability assays assessed by stress and short-term stability tests. The NP suspension was made at a concentration at 10^{-2} M. Lissamine™ rhodamine B 1,2-dihexadecanoyl-*sn*-glycero-3-phospho-ethanolamine, triethylammonium salt (rDHPE, Invitrogen, Carlsbad, CA) was used to label IDV–NP and appeared as red fluorescence (rDHPE-IDV-NP).

Monocyte solation, cultivation and viral infection

Human monocytes were obtained from leukopaks of HIV-1, 2 and hepatitis B seronegative donors and purified by countercurrent centrifugal elutriation (28). The University of Nebraska Medical Center Institutional Review Board approved the procedure. Cells were cultured with DMEM with 10% heat-inactivated pooled human serum, 1% glutamine, 10 mg/ml ciprofloxacin (Sigma Chemical Co., St. Louis, MO) and 1000 U/ml highly purified recombinant human macrophage colony stimulating factor (MCSF; a generous gift from Wyeth Inc., Cambridge, MA). Seven days after plating, MDM were infected with HIV-1_{ADA} at a multiplicity of infection (MOI) of 0.1 infectious viral particles/target cell (28). Culture medium was half-exchanged every 2–3 days. All viral stocks were tested and found to be free of mycoplasma and endotoxin contamination (Gen-Probe II; Gen-Probe, San Diego, CA).

Murine HIVE model

Four-six weeks-old male C.B.-17 SCID mice were purchased from The Charles River Laboratory (Wilmington, WA). Balb/c-Rag2-/-g_c-/- mice were bred at the University of Nebraska Medical Center for parallel studies of cell migration (29). Animal experiments were performed under strict observance of the National Institutes of Health and University of Nebraska guidelines for animal care. Animals were maintained in sterile microisolator cages. Briefly, all animals were anesthetized and placed in a stereotaxic apparatus (Stoetling Co., Wood Dale, IL) for intracranial injection. The animal's head was secured with earbars and mouthpiece. An injector with a 10 μl syringe was used for cell injections. The left hemisphere of each sham-operation animal (sham) received a total 5 μl of saline. Cell suspensions (5×10^5) with uninfected or HIV-1_{ADA}-infected MDM were injected into the brain's left hemisphere to induce HIVE in mice (30).

BMM isolation and cultivation

Male BALB/c mice (Charles River Laboratory, Inc.), 4–5 weeks of age were used as BMM donors. Briefly, the femur was removed, the bone marrow cells dissociated into single cell suspensions and cultured for 10 days supplemented with 1,000 units/ml of MCSF (Wyeth, Inc.). Cultured BMM proved to be 98% $CD11b^+$ by flow cytometric analysis using a FACS Calibur flow cytometer (BD Biosciences, San Jose, CA).

SPIO

HIVE SCID mice were injected with BMM containing super paramagnetic iron oxide (SPIO) particles (Feridex, Berlex Inc., Wayne, NJ). BMM were incubated at an SPIO concentration of 2mg/10^7 cells/ml for 2 h. This resulted in > 95% labeled cells as determined by Prussian blue stain. Cells were washed twice with DMEM, and each recipient mouse was injected intravenously through the tail vein with 150 μl containing 1×10^7 BMM loaded with SPIO (SPIO-BMM).

NIH-PA Author Manuscript

NIH-PA Author Manuscript

NIH-PA Author Manuscript

Drug treatment

BMM were incubated with rDHPE-IDV-NP at a concentration of 5×10^{-4} M for 12 h, and BMM packaged rDHPE-IDV-NP (rDHPE-IDV-NP-BMM) were washed twice with DMEM. A single dose of rDHPE-IDV-NP-BMM or IDV-NP was injected into each mouse intravenously through the tail vein.

IDV measurements

IDV-NP-BMM treated HIVE SCID mice (five in total per time point/group) were used to evaluate blood and brain tissue IDV levels at 1, 3, 7 and 14 days post-treatment. Macroscopic resections of the injected brain regions (regions including HIV-1 infected MDM), control hemispheres and whole blood were homogenized by sonication in 95% methanol (1 ml/2 g of tissue and 1 ml/0.5 ml of blood). Prepared tissue lysates were maintained at 4°C overnight and clarified by centrifugation at 14,000 x g for 10 min at 4°C. Supernatants were collected and analyzed by high performance liquid chromatography (HPLC, Waters Corp., Milford, MA) for determination of drug levels. Triplicate 20 μl aliquots of each sample were injected for HPLC analysis. IDV was separated from other tissue components using a mobile phase of (60/40) 25 mM postassium phosphate, pH 4.15: acetonitrile at 0.4 mL/min and a Waters YMC Octyl C8 column (3.0 × 150 mm). IDV was quantitated by comparison of peak area to that of a series of known IDV standards. Data are expressed as μg IDV/100 mg tissue or μg/mL in blood. Processing and analyses were validated using known concentrations of IDV and spiking drug into homogenized tissue samples from naive animals (5).

Confocal examination

For fluorescence evaluation of rDHPE-IDV-NP-BMM targeted migration to the regions of viral infection, brain tissue was collected on post-treatment day 3 after perfusion fixation with 4% paraformaldehyde in phosphate-buffered saline. Immunofluorescent staining was performed on sucrose-processed 25μm frozen brain sections. Antibodies to human specific vimentin-intermediate filaments (Vim, clone 3B4; Dako, Carpinteria, CA) were used for detection of human macrophages in the mouse brain. Antibody to HIV-1 p24 antigen (Dako) was utilized to determine the number of HIV-1-infected MDM. Rabbit polyclonal antibodies to ionized calcium-binding adapter molecule 1 (Iba-1, 1:500, Wako, Richmond, VA) was used to identify both MDM and murine microglia. Astrocytes were detected with antibodies against glial fibrillary acidic protein (GFAP, Dako). Antibodies to heavy chain (200 kDa) neurofilament (NF) antigens (Dako) were utilized to detect neurons. Fluorescent images were visualized with an LSM 410 confocal laser-scanning microscope (Zeiss, Goettinger, Germany) with argon/krypton at 488/568/647 nm. Quantification of rDHPE-IDV-NP-BMM levels was analyzed by using Image-Pro Plus (version 4.0, MediaCybernetics, Bethesda, MD). The red fluorescence area of rDHPE-IDV-NP-BMM was determined as a percentage of the total image area per microscopy field and calculated for a 0.1 mm window of tissue immediately surrounding the injection site.

Immunohistochemistry and image analyses

Sham, MDM and HIVE with or without IDV-NP-BMM treated mice were sacrificed at 7 and 14 days post-treatment. Each brain was paraffin-processed and cut to 5μm to identify the injection site. Immunohistochemistry was performed with the above antibodies. For location of SPIO-BMM, paraffin brain sections were stained with Prussian blue. Quantification of GFAP, Iba-1 and NF positive staining was achieved on serial coronal brain sections as a percentage of the total image area per microscopy field with a total of 30 fields (6 sections/mouse, five mice in each group) using Image-Pro Plus (MediaCybernetics). The absolute number of Vim^+ and HIV-1 $p24^+$cells, and MGC and MGC nuclei were counted under microscopy with 6 sections/mouse, five mice in each group.

NIH-PA Author Manuscript

NIH-PA Author Manuscript

NIH-PA Author Manuscript

Statistical analyses

The data was analyzed and comparisons performed using five mice/time point/group by two-tailed unpaired *t* test using Prism statistical software for MacIntosh (version 4.0, GraphPad Software, San Diego, CA). *P* values of < 0.05 were deemed significant.

Results

Uptake and cell release of IDV-NP

Our overarching idea is to use monocyte-macrophages as both carriers and extended depos for antiretroviral drugs for delivery to reservoirs for HIV and particularly the central nervous system (CNS). In a first step to test this idea we analyzed BMM uptake and release of IDV-NP using confocal microscopy and RP-HPLC tests. We used successive washes of adherent > 99% pure $CD68^+$ BMM cultures to displace surface bound NP and prove such displacement by confocal Z-scan analysis (27). NP visualized by fluorescence microscopy were seen within the cytoplasm of BMM and provided clear evidence that rDHPE-IDV-NP (red) were readily phagocytized within the macrophage (green, Figure 1A). rDHPE-IDV-NP (red) were observed in more than 98% of BMM. This was supported by HPLC tests performed after rDHPE-IDV-NP treatment (Figure 1B). Following sequential media changes, drug was released continuously as shown by HPLC tests and demonstrated both intracellular and extracellular levels of IDV. These progressively diminished over 7 days (Figure 1C).

Tracking BMM migration to diseased brain subregions

The next series of experiments examined the distributions of monocyte-macrophages after intravenous cell injections. To determine differences for BMM migration as a consequence of HIVE we performed replicate experiments with virus-infected and uninfected human MDM and sham-operated injections into subcortical (caudate and putamen) brain regions. In these experiments, the subcortical injection of HIV-1 infected human MDM induced a focal HIVE reflective of human HIVE (30). This included astrogliosis and microgliosis, loss of neurons and ongoing viral replication in affected brain regions as demonstrated by the presence of HIV-$1p24^+$ cells (Figure 2A). MDM and saline sham-operated mice were controls. Into these animals BMM carrying IDV NP were administered through the tail vein 24 hrs after brain injections. Mice were sacrificed on days 1, 3, 7 and 14 for histopathological analyses and assay of IDV drug levels. We reasoned that the neuroinflammatory responses induced by viral infection and in particular, HIVE, provided a biological system wherein blood-borne monocyte-macrophages carrying NP would ingress to diseased brain sites. Thus, BMM migration in diseased brain regions was measured. Initial experiments performed with BMM loaded with SPIO and administered intravenously to HIVE mice showed that the macrophages readily migrated to areas of HIVE as seen by Prussian blue staining (Figure 2A and C). This paralleled sites of reactive gliosis and HIV-1p24+ cells. No Prussian blue stained BMM were obtained in the contralateral hemispheres of either HIVE or sham-operated animals (Figure 2B and D). Neuropathological examinations confirmed that BMM target sites of ongoing viral replication (Figure 2A and C). The migration patterns of BMM were highly specific to sites of tissue injury, inflammation and viral growth.

HIV-1 infected macrophage neuroinflammatory responses elicit BMM brain transmigration

HIV-1 infection of brain macrophages is associated with ongoing viral infection, astrogliosis and microgliosis. This is seen where HIV-1p24, $GFAP^+$ and Iba-1^+ stained cells are linked with each other (Figure 3A–C). In Figure 2 it was demonstrated that BMM migration occurs readily toward neuroinflammatory sites. In murine HIVE, the association between such cell migration and neuroinflammation involves activation of astrocytes and microglia and consequent pro-inflammatory CNS responses (31–36). In order to determine whether BMM

NIH-PA Author Manuscript

NIH-PA Author Manuscript

NIH-PA Author Manuscript

carrying ART can migrate into HIVE affected brain regions we determined NP levels in brain 3 days following intravenous injection of rDHPE-IDV-NP-BMM. For these experiments one day after brain stereotactic injection with infected MDM, rDHPE-IDV-NP loaded BMM were injected intravenously through the tail vein. Brain tissue was examined in areas around the human MDM injection site. In HIVE mice, significant $GFAP^+$ astrogliosis (green, Figure 3A) and Iba-1^+ microglial responses (green, Figure 3B) were observed. Importantly, such neuroinflammatory responses were observed co-localized with rDHPE-IDV-NP-BMM (Figure 3C). In regards to specificity of these responses, BMM levels were reduced in MDM mice when compared in HIV mice. Moreover, few red fluorescence cells were detected in sham-operated brains (Figure 3A,B). In all animal groups no rDHPE-IDV-NP-BMM were found in the contralateral hemisphere. Few numbers of rDHPE-IDV-NP-BMM were seen in brains injected with uninfected MDM (supplemental figure 1).

Cell-based NP delivery affect IDV brain levels

To determine brain distribution of BMM loaded with nanoformulated IDV, the optical properties of red fluorescent rDHPE-IDV-NP were used. The images of brain sections reflect robust levels of BMM-rDHPE-IDV-NP (red) targeted in the areas of HIV-1 infection. Mouse-specific BMM $CD68^+$ cells (green, Figure 4A) were vehicles for IDV-NP delivery to the brain. BMM migrated to sites of HIVE. The rDHPE-IDV-NP-BMM (red) were concentrated around the virus-infected sites (Figure 4B) and colocalized with $CD68^+$ immunostaining (Figure 4A). Higher levels of $CD68^+$ BMM and rDHPE-IDV-NP-BMM were in HIVE brains when compared to uninfected MDM (supplemental figures) and sham controls (Figures 4A and B). Associations between productive viral infection and the presence of rDHPE-IDV-NP-BMM were easily seen indicating that viral infection and inflammatory responses induced BMM brain migration. The xenogenic responses to human MDM (supplemental figure 2) showed, in part, that rDHPE-IDV-NP entered the brain as a result of even modest neuroinflammatory responses. However, BMM migration was enhanced significantly by HIV-1 infection. These results suggest that ongoing HIV-1 infection of macrophages affected activation of astrocytes and microglia that in turn induced BMM CNS migration. In support of this idea was the fact that large numbers of rDHPE-IDV-NP-BMM were found in association with HIV-$1p24^+$ MDM (Figure 4B, green). Furthermore, HIV-1 infection of MDM served to increase the levels of $GFAP^+$ reactive astrocytes in the injected hemisphere of HIVE mice (Figure 4B, blue) when compared with uninfected MDM (supplemental Figure 2B) and sham-injected animals. The area of rDHPE-IDV-NP-BMM, determined by digital image analysis, was increased in HIVE mice ($p < 0.01$) compared to both uninfected MDM and sham controls (Figure 5A). Likewise numbers of $CD68^+$ BMM were also increased in HIVE mice ($p < 0.01$) compared to sham-operated controls (Figure 5B). Altogether, these findings support targeted migration of IDV-NP-BMM into areas of active HIV-1 infection and neuroinflammation.

To validate these findings of selective drug-carried BMM into brain diseased areas, we administered by intravenous injection a single dose of IDV-NP-BMM to HIVE mice and determined IDV levels in tissues from the caudate and putamen on days 1, 3, 7 and 14 after treatment. Quantifiable amounts of IDV were obtained in blood (Figure 5C) and comparable levels of IDV in diseased (ipsilateral) and control (contralateral) hemispheres (Figure 5D) were assayed by RP-HPLC. One IDV-NP-BMM treatment elicited sustained drug levels in blood for up to 14 days (Figure 5C). More importantly, IDV-NP-BMM delivery attained higher drug levels at day 14 in the ipsilateral than contralateral hemisphere of HIVE mice (Figure 5D). These results confirmed that NP-IDV was successfully delivered into the brain by packaging into BMM, thus providing proof-of-concept for therapeutic drug delivery in animal models of human disease.

NIH-PA Author Manuscript

NIH-PA Author Manuscript

NIH-PA Author Manuscript

Antiretroviral responses of IDV-NP-BMM

We previously demonstrated that after IDV-NP-BMM administration long-term viral suppression and increased $CD4^+$ T-cell levels were achieved (5). A single administration of IDV-NP-BMM achieved drug concentrations 4–10 fold higher in plasma and lymph tissues and were more sustained than those attained with a single bolus of non-formulated IDV. In order to validate our results, we used Balb/c-Rag2-/-g_c-/- mice which provided long-term engraftment of human MDM in murine environment (29). To reach a therapeutic IDV concentration and determine antiviral efficacy in brains, IDV-NP-BMM was administered to HIVE mice; replicate animals were untreated. After 7 and 14 days, the extent of HIV-1 infection in the brains was determined. Immunostaining of brain sections showed that human Vim^+ MDM (Figure 6A) co-located with activation of $GFAP^+$ astrocytes in HIVE mice. Immunohistochemistry determined the levels of MDM reconstitution and viral infection by counting the absolute number of Vim^+ and HIV-$1p24^+$ MDM in brain sections. The absolute number of Vim^+ and HIV-1 $p24^+$ MDM were counted as cells/section in 6 sections per mouse as shown in table 1. To determine the effects of IDV-NP-BMM administration on long-term antiviral responses, HIV-$1p24^+$ cells were assessed as a percent of total human MDM (Vim^+). With a single treatment of IDV-NP-BMM, decreased numbers of HIV-1 infected cells were observed in IDV-NP-BMM treated HIVE mice as compared to untreated animals (Figure 6B). This was significantly apparent in brain sections ($p < 0.01$) on days 7 and 14, reflecting a long-term robust antiretroviral response elicited by IDV-NP-BMM. Based on the observation of a reduction in HIV-$1p24^+$ cells in the IDV-NP-BMM treated HIVE mice, we studied MGC formation in brain sections found exclusively in injection sites where HIV-$1p24^+$ cells were seen. Brain histopathology of untreated HIVE mice is shown (Figure 6A). Visualization of MGC showed large numbers of nuclei within cells shown by arrowheads. MGC and nuclei were counted using absolute numbers in brain sections at day 7 and 14. The numbers of MGC were 11.9 ± 2.7 and 7.2 ± 4.08 (counts/section) on day 7, and 5.1 ± 1.6 and 1.7 ± 1.2 (counts/section) on day 14 in untreated and IDV-NP-BMM treated HIVE mice, respectively. Mean numbers of nuclei within MGCs were 13.8 ± 2.8 and 7.1 ± 2.0 on day 7, and 7.4 ± 0.7 and 4.9 ± 0.6 on day 14 in untreated and IDV-NP-BMM treated HIVE mice, respectively. Significantly decreased numbers of MGC (both $p < 0.01$) and nuclei ($p < 0.05$ and $p < 0.01$) on day 7 and 14 were observed following IDV-NP-BMM treatment. Figure 6A also demonstrated changes in the MDM phenotype (Vim^+). A stalk containing nucleus became elongated in untreated HIVE mice (Figure 6A). IDV-NP-BMM treatment limited MGC formation. Based on a significantly reduced HIV-1 p24 expression in treated group, we determined that MGC formation was linked to HIV-1 infection. The levels of MGCs was significantly decreased when assayed by ratios of MGC/total Vim^+ MDM (Figure 6C) in IDV-NP-BMM treated HIVE brains.

Preliminary toxicology studies

To investigate the potential toxicity of IDV-NP-BMM at the delivery site and more extensively throughout the brain, histopathological analysis of brain sections was used to examine neuronal integrity in SCID mice injected in the brain with human MDM (supplemental Figure 2C) or HIV-1 infected MDM. Sham operated animals served as controls. In order to separate neuronal injury induced as a consequence of viral infection and/or inflammation caused by xenogenic MDM (Supplemental figure 2). Three groups of mice (sham control, MDM and HIVE) were used to determine whether any neurotoxicity was induced by the nanoformulations themselves. MDM are known to induce inflammatory responses and are capable of promoting BMM migration into the brain. Immunostaining for NF was performed in brain sections to identify neuronal loss. Confocal microscopy images demonstrated IDV-NP-BMM (red) migration into areas of MDM with or without HIV-1 infection (Figure 3–Figure 7). HIV-1 infection and ongoing inflammatory responses shown as HIV-1 p24 expressions, $GFAP^+$ astrogliosis and Iba-1 microgliosis (Figure, 3, Figure 4 and Figure 6) were revealed in response to the needle

NIH-PA Author Manuscript

NIH-PA Author Manuscript

NIH-PA Author Manuscript

track in sham-operated animals. Immunostaining for NF (green, Figure 7A) was performed in brain sections to identify neuronal loss in HIVE diseased areas with or without IDV-NP-BMM treatment (Figure 7A). Indeed, abnormal accumulation of NF^+ neuron body was located in the diseased areas where ongoing inflammatory and viral infection was occurring. Confocal microscopy images demonstrated IDV-NP-BMM (red) migration into diseased areas with ongoing HIV-1 infection (Figure 7A) and/or inflammatory responses (Supplemental Figure 2C). Sham control revealed few rDHPE positive spots. NF staining loss was seen in HIV-1 infected MDM occupied sites and surrounding areas. Indeed, abnormal accumulation of phosphorylated NF^+ (p-NF) in the neuron body was observed in both MDM and HIVE mice with or without IDV-NP-BMM treatment. NF expression (Figure 7A–C) and p-NF^+ neuron bodies were evaluated. Image quantitation of neuronal damage (NF^+ axons) and p-NF^+ neuron bodies demonstrates that NF expression (Figure 7B) was no different in the IDV-NP-BMM treated HIVE mice compared to the untreated group. The numbers of accumulated p-NF^+ neuron bodies together with $GFAP^+$ and Iba-1^+ astrocytes and microglia showed (Figure 7C–E) no changes amongst treated and untreated mice.

Discussion

Invasion of HIV into the CNS occurs early after viral exposure and during the development of a seroconversion reaction (37,38). Disease, however, occurs years later as a consequence of chronic viral infection of brain MP including blood-borne perivascular macrophages and microglia, culminating in neuronal injury and death (39–43). Interestingly, these same MP cells carry the virus from the periphery into the brain and serve as sources of neuroinflammatory mediators. Such an inflammatory response generates chemokine gradients, encouraging additional monocyte-macrophages to enter the brain as well as providing a rich source of neurotoxins (42–46). Cognitive, motor and behavioral abnormalities occurs as a consequence of such pathogenic events and are fueled by continuous viral growth in the face of damaged or lost adaptive immunity (47–49). We reasoned that improving brain penetration of ART would affect the tempo and progression of disease by controlling viral growth. To accomplish this we took advantage of the ingress of monocyte-macrophages from the blood to the brain operative in disease. Such cell ingress correlates with disease severity (50–52) and could be harnessed for therapeutic gain. By using BMM as ART carriers, the actual entry of disease-causing cells could be used to improve disease outcomes. BMM loaded with IDV-NP readily penetrate the BBB, enter brain subregions and migrate to disease sites of continuous viral replication and neuroinflammation. These results provide further validation for the use of macrophage-drug delivery systems to combat HIV infection (5,27,53,54).

ART can restore cognitive function while limiting neural damage in HIV-1 infected people (11,55,56). Indeed, HIV load present in cerebrospinal fluid (CSF) and the number of immune competent macrophages correlate with the degree of cognitive deficits and most notably, the numbers of $CD4^+$ T lymphocytes (57–61). This supports the idea that sustained penetration of ART across the BBB improves clinical neurological outcomes (41,62). Indeed, ART can prolong life expectancy and restore immune activities, resulting in improved surveillance of virus and reductions of opportunistic infections and primary CNS lymphomas (63–66). In contrast, ineffective use of ART or its reduced brain penetration could contribute to viral mutation and sustained HIV replication within the brain sanctuary (67). Significant evidence shows that viral resistance patterns within the CSF compartment are distinct from that found in plasma (68,69). Moreover, virologic CSF suppression is associated with ART brain penetrance (70). Nonetheless, the BBB limits the numbers of drugs that readily enter the CNS. Therefore, drugs that enter the CNS and suppress ongoing viral replication are believed to provide the best clinical outcomes. These observations, taken together, indicated that the development of a novel antiretroviral drug delivery system to improve the CNS penetration and ART efficacy is important.

NIH-PA Author Manuscript

NIH-PA Author Manuscript

NIH-PA Author Manuscript

Our laboratory and those of others developed macrophage-based nanoformulations to treat neuroAIDS and other neurodegenerative diseases (5,27,53,54,71). Such macrophage drug carriage was shown to enhance local drug concentration, elicit limited systemic side effects, and affect ART efficacy in rodent models of HIV infection (5). Our previous works with the HIV-1 protease inhibitor IDV showed that IDV-NP carried in BMM could positively affect pharmacokinetic drug delivery and improve tissue distribution in laboratory and animal models of HIV disease (5,27). The current results extend these observations significantly by demonstrating the biodistribution and antiretroviral activity of IDV-NP-BMM within CNS tissue compartments exhibiting active HIV-1-induced disease. Levels of IDV in HIV-1 infected brain areas were significantly increased and extended to 14 days with a single dosage of IDV-NP-BMM treatment in comparison to intravenous administered IDV. Compared to control hemispheres, a significantly high level of IDV was obtained in diseased hemispheres on day 14.

Nanotechnology has revolutionized modern-day pharmacology (72–76). The ability to alter carrier size, shape and composition allows incorporation of drugs with a broad range of physical and biochemical properties (77). Nanoformulations have a number of advantages over conventional oral or intravenous drug systems in their capacity to increase systemic bioavailability and solubility, and slow drug degradation. Our macrophage-based system expands these observations even further in a number of divergent ways. *First*, monocyte-macrophages can carry drugs across the BBB to target disease areas and improve local drug distribution. *Second*, the macrophage delivery system relies on natural pathogenic processes elicited during inflammatory responses. These responses serve to target disease sites of active HIV-1 replication. In this way, there is a natural control for drug penetration that is based on disease severity. *Third*, monthly dosing positively affects therapeutic outcomes by prolonging the presence of local drug, and in so doing, reducing opportunities for viral mutation and disease (5).

Macrophages have received significant attention for their role as drug carriers (78,79). However, relatively few *in vivo* studies have assessed the ability of the macrophage-drug delivery system to target migration to disease sites. We developed a novel method using macrophages for delivery of IDV-NP across the BBB to improve anti-viral efficacy and enhance brain drug distribution. The advantages of BMM as a carrier of NP for antiretroviral drugs include an effective and systemic delivery system *in vivo* to track cell migration and to utilize therapeutic activities. The significance of this work is reflected by its interdisciplinary approaches to strategizing crossing of the BBB, targeting migration, improving brain drug levels and assessing antiretroviral responses. Based on the numbers of blood borne macrophages that have entered affected brain regions and taking into account that > 98% of the cells carry drugs (5), the IDV levels observed in brain were lower than would be expected. While measures of the drug in wedge brain dissections provide proof-of-concept, absolute drug levels are diluted by the necessary inclusion of surrounding unaffected tissues in drug analysis. Thus, the precise amount of drug delivered into areas of active disease will require microdissection of encephalitic brain subregions. This remains a major and ongoing focus of our own research efforts. Improvements of CNS drug penetration, targeted delivery, single dosage administration, economy, sustained release and drug bioavailability can assuredly make nanoART attractive for human use. This study is certainly important as it represents a new direction for effective treatment of one of the most debilitating complications of HIV-1 infection, namely, cognitive impairment.

Supplementary Material

Refer to Web version on PubMed Central for supplementary material.

NIH-PA Author Manuscript

NIH-PA Author Manuscript

NIH-PA Author Manuscript

Acknowledgements

The authors gratefully thank Robin Taylor for critical reading of the manuscript and outstanding computer support; Dr. Larisa Y Poluektova, who supplied the Balb/c-Rag2-/-g_c-/- mice; and Mr. Michael T. Jacobsen and Ms. Janice Taylor, who provided confocal microscopic assistance.

References

1. Antinori A, Arendt G, Becker JT, Brew BJ, Byrd DA, Cherner M, Clifford DB, Cinque P, Epstein LG, Goodkin K, Gisslen M, Grant I, Heaton RK, Joseph J, Marder K, Marra CM, McArthur JC, Nunn M, Price RW, Pulliam L, Robertson KR, Sacktor N, Valcour V, Wojna VE. Updated research nosology for HIV-associated neurocognitive disorders. Neurology 2007;69:1789–1799. [PubMed: 17914061]
2. Dickson DW. Multinucleated giant cells in acquired immunodeficiency syndrome encephalopathy. Origin from endogenous microglia? Arch Pathol Lab Med 1986;110:967–968. [PubMed: 3533004]
3. Budka H. Multinucleated giant cells in brain: a hallmark of the acquired immune deficiency syndrome (AIDS). Acta Neuropathol 1986;69:253–258. [PubMed: 3962603]
4. Navia BA, Cho ES, Petito CK, Price RW. The AIDS dementia complex: II. Neuropathology. Ann Neurol 1986;19:525–535. [PubMed: 3014994]
5. Dou H, Destache CJ, Morehead JR, Mosley RL, Boska MD, Kingsley J, Gorantla S, Poluektova L, Nelson JA, Chaubal M, Werling J, Kipp J, Rabinow B, Gendelman HE. Development of a macrophage-based nanoparticle system for antiretroviral drug delivery. Blood 2006;108:2827–2835. [PubMed: 16809617]
6. Liu Y, UM DH, Banerjee R, Grotepas CB, Stone D Rabinow BE, Gendelman HE, Boska MD. Ingress of blood-borne macrophages across the blood-brain barrier in murine HIV-1 encephalitis. Journal of Neuroimmunology. 2008
7. D'Amico R, Sarkar S, Yusuff J, Azar E, Perlman DC. Immune reconstitution after potent antiretroviral therapy in AIDS patients with progressive multifocal leukoencephalopathy. Scand J Infect Dis 2007;39:347–350. [PubMed: 17454900]
8. Van Rie A, Harrington PR, Dow A, Robertson K. Neurologic and neurodevelopmental manifestations of pediatric HIV/AIDS: a global perspective. Eur J Paediatr Neurol 2007;11:1–9. [PubMed: 17137813]
9. Trujillo JR, Jaramillo-Rangel G, Ortega-Martinez M, Penalva de Oliveira AC, Vidal JE, Bryant J, Gallo RC. International NeuroAIDS: prospects of HIV-1 associated neurological complications. Cell Res 2005;15:962–969. [PubMed: 16354575]
10. Spudich SS, Nilsson AC, Lollo ND, Liegler TJ, Petropoulos CJ, Deeks SG, Paxinos EE, Price RW. Cerebrospinal fluid HIV infection and pleocytosis: relation to systemic infection and antiretroviral treatment. BMC Infect Dis 2005;5:98. [PubMed: 16266436]
11. Enzensberger W, von Giesen HJ. Antiretroviral therapy (ART) from a neurological point of view. German Neuro-AIDS study group (DNAA). Eur J Med Res 1999;4:456–462. [PubMed: 10585300]
12. Smit TK, Brew BJ, Tourtellotte W, Morgello S, Gelman BB, Saksena NK. Independent evolution of human immunodeficiency virus (HIV) drug resistance mutations in diverse areas of the brain in HIV-infected patients, with and without dementia, on antiretroviral treatment. J Virol 2004;78:10133–10148. [PubMed: 15331746]
13. Antinori A, Perno CF, Giancola ML, Forbici F, Ippolito G, Hoetelmans RM, Piscitelli SC. Efficacy of cerebrospinal fluid (CSF)-penetrating antiretroviral drugs against HIV in the neurological compartment: different patterns of phenotypic resistance in CSF and plasma. Clin Infect Dis 2005;41:1787–1793. [PubMed: 16288405]
14. Wegner SA, Brodine SK, Mascola JR, Tasker SA, Shaffer RA, Starkey MJ, Barile A, Martin GJ, Aronson N, Emmons WW, Stephan K, Bloor S, Vingerhoets J, Hertogs K, Larder B. Prevalence of genotypic and phenotypic resistance to antiretroviral drugs in a cohort of therapy-naive HIV-1 infected US military personnel. Aids 2000;14:1009–1015. [PubMed: 10853983]
15. Garcia F, Alonso MM, Romeu J, Knobel H, Arrizabalaga J, Ferrer E, Dalmau D, Ruiz I, Vidal F, Frances A, Segura F, Gomez-Sirvent JL, Cruceta A, Clotet B, Pumarola T, Gallart T, O'Brien WA, Miro JM, Gatell JM. Comparison of immunologic restoration and virologic response in plasma, tonsillar tissue, and cerebrospinal fluid in HIV-1-infected patients treated with double versus triple

NIH-PA Author Manuscript

NIH-PA Author Manuscript

NIH-PA Author Manuscript

antiretroviral therapy in very early stages: The Spanish EARTH-2 Study. Early Antiretroviral Therapy Study. J Acquir Immune Defic Syndr 2000;25:26–35. [PubMed: 11064501]

16. Flandre P, Chappey C, Marcelin A, Ryan K, Maa J, Bates M, Seekins D, Bernard M, C V, Molina J. Phenotypic susceptibility to didanosine is associated with antiviral activity in treatment-experienced patients with HIV-1 infection. J Infect Dis. J Infect Dis 2007:392–398.
17. Doualla-Bell F, Turner D, Loemba H, Petrella M, Brenner B, Wainberg MA. HIV drug resistance and optimization of antiviral treatment in resource-poor countries. Med Sci (Paris) 2004;20:882–886. [PubMed: 15461965]
18. Aweeka F, Jayewardene A, Staprans S, Bellibas SE, Kearney B, Lizak P, Novakovic-Agopian T, Price RW. Failure to detect nelfinavir in the cerebrospinal fluid of HIV-1--infected patients with and without AIDS dementia complex. J Acquir Immune Defic Syndr Hum Retrovirol 1999;20:39–43. [PubMed: 9928728]
19. Resch W, Parkin N, Watkins T, Harris J, Swanstrom R. Evolution of human immunodeficiency virus type 1 protease genotypes and phenotypes in vivo under selective pressure of the protease inhibitor ritonavir. J Virol 2005;79:10638–10649. [PubMed: 16051856]
20. Jacobsen H, Hanggi M, Ott M, Duncan IB, Owen S, Andreoni M, Vella S, Mous J. In vivo resistance to a human immunodeficiency virus type 1 proteinase inhibitor: mutations, kinetics, and frequencies. J Infect Dis 1996;173:1379–1387. [PubMed: 8648209]
21. Zhang H, Dornadula G, Wu Y, Havlir D, Richman DD, Pomerantz RJ. Kinetic analysis of intravirion reverse transcription in the blood plasma of human immunodeficiency virus type 1-infected individuals: direct assessment of resistance to reverse transcriptase inhibitors in vivo. J Virol 1996;70:628–634. [PubMed: 8523584]
22. Stockmann M, Schmitz H, Fromm M, Schmidt W, Pauli G, Scholz P, Riecken EO, Schulzke JD. Mechanisms of epithelial barrier impairment in HIV infection. Ann N Y Acad Sci 2000;915:293–303. [PubMed: 11193591]
23. Thomas SA. Anti-HIV drug distribution to the central nervous system. Curr Pharm Des 2004;10:1313–1324. [PubMed: 15134483]
24. Loscher W, Potschka H. Drug resistance in brain diseases and the role of drug efflux transporters. Nat Rev Neurosci 2005;6:591–602. [PubMed: 16025095]
25. Fromm MF. P-glycoprotein: a defense mechanism limiting oral bioavailability and CNS accumulation of drugs. Int J Clin Pharmacol Ther 2000;38:69–74. [PubMed: 10706193]
26. Gibbs JE, Rashid T, Thomas SA. Effect of transport inhibitors and additional anti-HIV drugs on the movement of lamivudine (3TC) across the guinea pig brain barriers. J Pharmacol Exp Ther 2003;306:1035–1041. [PubMed: 12766261]
27. Dou H, Morehead J, Destache CJ, Kingsley JD, Shlyakhtenko L, Zhou Y, Chaubal M, Werling J, Kipp J, Rabinow BE, Gendelman HE. Laboratory investigations for the morphologic, pharmacokinetic, and antiretroviral properties of indinavir nanoparticles in human monocyte-derived macrophages. Virology 2007;358:148–158. [PubMed: 16997345]
28. Gendelman HE, Orenstein JM, Martin MA, Ferrua C, Mitra R, Phipps T, Wahl LA, Lane HC, Fauci AS, Burke DS, et al. Efficient isolation and propagation of human immunodeficiency virus on recombinant colony-stimulating factor 1-treated monocytes. J Exp Med 1988;167:1428–1441. [PubMed: 3258626]
29. Gorantla S, Sneller H, Walters L, Sharp JG, Pirruccello SJ, West JT, Wood C, Dewhurst S, Gendelman HE, Poluektova L. Human immunodeficiency virus type 1 pathobiology studied in humanized BALB/c-Rag2-/-gammac-/- mice. J Virol 2007;81:2700–2712. [PubMed: 17182671]
30. Persidsky Y, Buttini M, Limoges J, Bock P, Gendelman HE. An analysis of HIV-1-associated inflammatory products in brain tissue of humans and SCID mice with HIV-1 encephalitis. J Neurovirol 1997;3:401–416. [PubMed: 9475112]
31. Peterson KE, Du M. Innate immunity in the pathogenesis of polytropic retrovirus infection in the central nervous system. Immunol Res 2009;43(1–3):149–159. [PubMed: 18818884]
32. Huang D, Han Y, Rani MR, Glabinski A, Trebst C, Sorensen T, Tani M, Wang J, Chien P, O 'Bryan B, Bielecki B, Zhou ZL, Majumder S, Ransohoff RM. Chemokines and chemokine receptors in inflammation of the nervous system: manifold roles and exquisite regulation. Immunol Rev 2000;177:52–67. [PubMed: 11138785]

NIH-PA Author Manuscript NIH-PA Author Manuscript NIH-PA Author Manuscript

33. Speth C, Dierich MP, Sopper S. HIV-infection of the central nervous system: the tightrope walk of innate immunity. Mol Immunol 2005;42:213–228. [PubMed: 15488609]
34. DeLeo JA, Tanga FY, Tawfik VL. Neuroimmune activation and neuroinflammation in chronic pain and opioid tolerance/hyperalgesia. Neuroscientist 2004;10:40–52. [PubMed: 14987447]
35. Belmadani A, Tran PB, Ren D, Miller RJ. Chemokines regulate the migration of neural progenitors to sites of neuroinflammation. J Neurosci 2006;26:3182–3191. [PubMed: 16554469]
36. Ramirez SH, Heilman D, Morsey B, Potula R, Haorah J, Persidsky Y. Activation of peroxisome proliferator-activated receptor gamma (PPARgamma) suppresses Rho GTPases in human brain microvascular endothelial cells and inhibits adhesion and transendothelial migration of HIV-1 infected monocytes. J Immunol 2008;180:1854–1865. [PubMed: 18209083]
37. Gray F, Scaravilli F, Everall I, Chretien F, An S, Boche D, Adle-Biassette H, Wingertsmann L, Durigon M, Hurtrel B, Chiodi F, Bell J, Lantos P. Neuropathology of early HIV-1 infection. Brain Pathol 1996;6:1–15. [PubMed: 8866743]
38. Wingertsmann L, Chretien F, Authier FJ, Paraire F, Durigon M, Gray F. Central nervous system lesions in the early stages of HIV infection. Arch Anat Cytol Pathol 1997;45:106–117. [PubMed: 9382601]
39. Gray F. Lesions of the central nervous system in the early stages of human immunodeficiency virus infection. Rev Neurol (Paris) 1997;153:629–640. [PubMed: 9686250]
40. Williams K, Alvarez X, Lackner AA. Central nervous system perivascular cells are immunoregulatory cells that connect the CNS with the peripheral immune system. Glia 2001;36:156–164. [PubMed: 11596124]
41. Epstein LG. HIV neuropathogenesis and therapeutic strategies. Acta Paediatr Jpn 1998;40:107–111. [PubMed: 9581298]
42. Griffin DE. Cytokines in the brain during viral infection: clues to HIV-associated dementia. J Clin Invest 1997;100:2948–2951. [PubMed: 9399939]
43. Tong N, Perry SW, Zhang Q, James HJ, Guo H, Brooks A, Bal H, Kinnear SA, Fine S, Epstein LG, Dairaghi D, Schall TJ, Gendelman HE, Dewhurst S, Sharer LR, Gelbard HA. Neuronal fractalkine expression in HIV-1 encephalitis: roles for macrophage recruitment and neuroprotection in the central nervous system. J Immunol 2000;164:1333–1339. [PubMed: 10640747]
44. Garzino-Demo A, DeVico AL, Gallo RC. Chemokine receptors and chemokines in HIV infection. J Clin Immunol 1998;18:243–255. [PubMed: 9710741]
45. Kaul M, Lipton SA. Mechanisms of neuroimmunity and neurodegeneration associated with HIV-1 infection and AIDS. J Neuroimmune Pharmacol 2006;1:138–151. [PubMed: 18040780]
46. Kaul M, Lipton SA. Mechanisms of neuronal injury and death in HIV-1 associated dementia. Curr HIV Res 2006;4:307–318. [PubMed: 16842083]
47. Epstein LG, Gelbard HA. HIV-1-induced neuronal injury in the developing brain. J Leukoc Biol 1999;65:453–457. [PubMed: 10204573]
48. Cherner M, Cysique L, Heaton RK, Marcotte TD, Ellis RJ, Masliah E, Grant I. Neuropathologic confirmation of definitional criteria for human immunodeficiency virus-associated neurocognitive disorders. J Neurovirol 2007;13:23–28. [PubMed: 17454445]
49. Anderson E, Zink W, Xiong H, Gendelman HE. HIV-1-associated dementia: a metabolic encephalopathy perpetrated by virus-infected and immune-competent mononuclear phagocytes. J Acquir Immune Defic Syndr 2002;31:S43–S54. [PubMed: 12394782]
50. Minagar A, Shapshak P, Fujimura R, Ownby R, Heyes M, Eisdorfer C. The role of macrophage/microglia and astrocytes in the pathogenesis of three neurologic disorders: HIV-associated dementia, Alzheimer disease, and multiple sclerosis. J Neurol Sci 2002;202:13–23. [PubMed: 12220687]
51. Power C, Johnson RT. HIV-1 associated dementia: clinical features and pathogenesis. Can J Neurol Sci 1995;22:92–100. [PubMed: 7627922]
52. Glass JD, Fedor H, Wesselingh SL, McArthur JC. Immunocytochemical quantitation of human immunodeficiency virus in the brain: correlations with dementia. Ann Neurol 1995;38:755–762. [PubMed: 7486867]
53. Gorantla S, Dou H, Boska M, Destache CJ, Nelson J, Poluektova L, Rabinow BE, Gendelman HE, Mosley RL. Quantitative magnetic resonance and SPECT imaging for macrophage tissue migration and nanoformulated drug delivery. J Leukoc Biol 2006;80:1165–1174. [PubMed: 16908517]

NIH-PA Author Manuscript NIH-PA Author Manuscript NIH-PA Author Manuscript

54. Kingsley J, Dou H, Morehead J, Rabinow B, Gendelman H, Destache C. Nanotechnology: a focus on Nanoparticles as a Drug delivery System. J neuroimmune Pharmacol 2006;1:340–350. [PubMed: 18040810]
55. Anthony IC, Ramage SN, Carnie FW, Simmonds P, Bell JE. Accelerated Tau deposition in the brains of individuals infected with human immunodeficiency virus-1 before and after the advent of highly active antiretroviral therapy. Acta Neuropathol 2006;111:529–538. [PubMed: 16718349]
56. Stingl G. Antiretroviral therapy in HIV-1-infected persons: concepts and strategies. Curr Probl Dermatol 1989;18:250–268. [PubMed: 2663369]
57. Goodkin K, Vitiello B, Lyman WD, Asthana D, Atkinson JH, Heseltine PN, Molina R, Zheng W, Khamis I, Wilkie FL, Shapshak P. Cerebrospinal and peripheral human immunodeficiency virus type 1 load in a multisite, randomized, double-blind placebo-controlled trial of D-Ala1-peptide T-amide for HIV-1-associated cognitive-motor impairment. J Neurovirol 2006;12:178–189. [PubMed: 16877299]
58. Vitiello B, Goodkin K, Ashtana D, Shapshak P, Atkinson JH, Heseltine PN, Eaton E, Heaton R, Lyman WD. HIV-1 RNA concentration and cognitive performance in a cohort of HIV-positive people. Aids 2007;21:1415–1422. [PubMed: 17589187]
59. Wiley CA, Lopresti BJ, Becker JT, Boada F, Lopez OL, Mellors J, Meltzer CC, Wisniewski SR, Mathis CA. Positron emission tomography imaging of peripheral benzodiazepine receptor binding in human immunodeficiency virus-infected subjects with and without cognitive impairment. J Neurovirol 2006;12:262–271. [PubMed: 16966217]
60. Rosci MA, Pigorini F, Bernabei A, Pau FM, Volpini V, Merigliano DE, Meligrana MF. Methods for detecting early signs of AIDS dementia complex in asymptomatic HIV-1-infected subjects. Aids 1992;6:1309–1316. [PubMed: 1361744]
61. Royal W 3rd, Selnes OA, Concha M, Nance-Sproson TE, McArthur JC. Cerebrospinal fluid human immunodeficiency virus type 1 (HIV-1) p24 antigen levels in HIV-1-related dementia. Ann Neurol 1994;36:32–39. [PubMed: 7912918]
62. Berger JR, Avison M. The blood brain barrier in HIV infection. Front Biosci 2004;9:2680–2685. [PubMed: 15358591]
63. Cao YZ, Lu HZ. Care of HIV-infected patients in China. Cell Res 2005;15:883–890. [PubMed: 16354564]
64. Hoffmann C, Tabrizian S, Wolf E, Eggers C, Stoehr A, Plettenberg A, Buhk T, Stellbrink HJ, Horst HA, Jager H, Rosenkranz T. Survival of AIDS patients with primary central nervous system lymphoma is dramatically improved by HAART-induced immune recovery. Aids 2001;15:2119–2127. [PubMed: 11684931]
65. Antinori A, Cingolani A, Alba L, Ammassari A, Serraino D, Ciancio BC, Palmieri F, De Luca A, Larocca LM, Ruco L, Ippolito G, Cauda R. Better response to chemotherapy and prolonged survival in AIDS-related lymphomas responding to highly active antiretroviral therapy. Aids 2001;15:1483–1491. [PubMed: 11504980]
66. Skiest DJ, Crosby C. Survival is prolonged by highly active antiretroviral therapy in AIDS patients with primary central nervous system lymphoma. Aids 2003;17:1787–1793. [PubMed: 12891064]
67. Lambotte O, Deiva K, Tardieu M. HIV-1 persistence, viral reservoir, and the central nervous system in the HAART era. Brain Pathol 2003;13:95–103. [PubMed: 12580549]
68. Saez-Llorens X, Castrejon de Wong MC, Castano E, de Suman O, Baez de Ulloa C, Redondo W, Espino M. Clinical and virological correlation between the cerebrospinal fluid and blood of HIV-infected children. Rev Med Panama 2001;26:13–18. [PubMed: 16161718]
69. Eggers C, Hertogs K, Sturenburg HJ, van Lunzen J, Stellbrink HJ. Delayed central nervous system virus suppression during highly active antiretroviral therapy is associated with HIV encephalopathy, but not with viral drug resistance or poor central nervous system drug penetration. Aids 2003;17:1897–1906. [PubMed: 12960822]
70. De Luca A, Ciancio BC, Larussa D, Murri R, Cingolani A, Rizzo MG, Giancola ML, Ammassari A, Ortona L. Correlates of independent HIV-1 replication in the CNS and of its control by antiretrovirals. Neurology 2002;59:342–347. [PubMed: 12177366]

NIH-PA Author Manuscript

NIH-PA Author Manuscript

NIH-PA Author Manuscript

71. Batrakova EV, Li S, Reynolds AD, Mosley RL, Bronich TK, Kabanov AV, Gendelman HE. A macrophage-nanozyme delivery system for Parkinson's disease. Bioconjug Chem 2007;18:1498–1506. [PubMed: 17760417]

72. Jain KK. The role of nanobiotechnology in drug discovery. Drug Discov Today 2005;10:1435–1442. [PubMed: 16243263]

73. Jain KK. Nanotechnology-based drug delivery for cancer. Technol Cancer Res Treat 2005;4:407–416. [PubMed: 16029059]

74. Michaelis M, Matousek J, Vogel JU, Slavik T, Langer K, Cinatl J, Kreuter J, Schwabe D. Bovine seminal ribonuclease attached to nanoparticles made of polylactic acid kills leukemia and lymphoma cell lines in vitro. Anticancer Drugs 2000;11:369–376. [PubMed: 10912953]

75. Xing X, He X, Peng J, Wang K, Tan W. Uptake of silica-coated nanoparticles by HeLa cells. J Nanosci Nanotechnol 2005;5:1688–1693. [PubMed: 16245529]

76. Varela MC, Guzman M, Molpeceres J, del Rosario Aberturas M, Rodriguez-Puyol D, Rodriguez-Puyol M. Cyclosporine-loaded polycaprolactone nanoparticles: immunosuppression and nephrotoxicity in rats. Eur J Pharm Sci 2001;12:471–478. [PubMed: 11231114]

77. Chan WC. Bionanotechnology progress and advances. Biol Blood Marrow Transplant 2006;12:87–91. [PubMed: 16399591]

78. Burke WJ. 3,4-dihydroxyphenylacetaldehyde: a potential target for neuroprotective therapy in Parkinson's disease. Curr Drug Targets CNS Neurol Disord 2003;2:143–148. [PubMed: 12769806]

79. Basu MK, Lala S. Macrophage specific drug delivery in experimental leishmaniasis. Curr Mol Med 2004;4:681–689. [PubMed: 15357216]

NIH-PA Author Manuscript
NIH-PA Author Manuscript
NIH-PA Author Manuscript

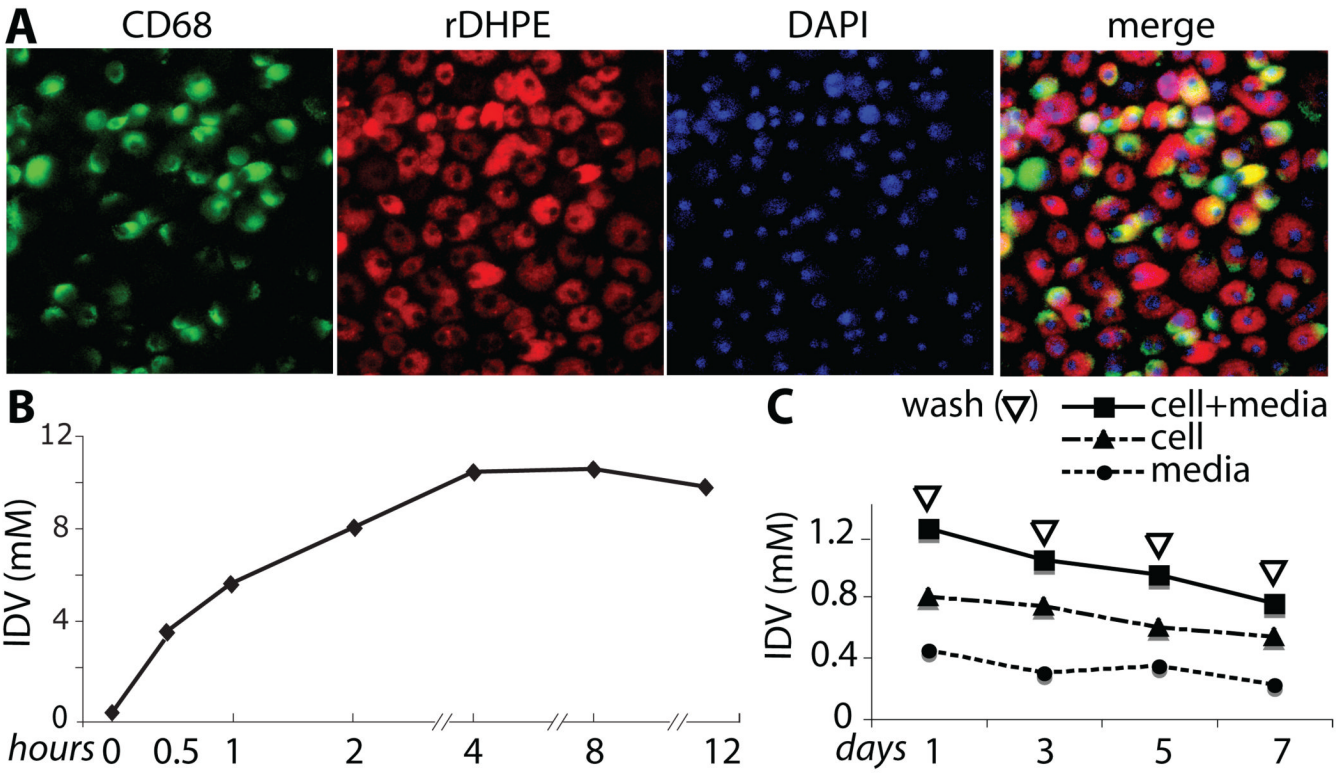

FIGURE 1.

Cellular NP uptake and IDV release. Fluorescence microscopy imaging of rDHPE-IDV-NP (red) treated BMM (green, $CD68^{+}$) demonstrating intracellular localization of IDV-NP (A). Ingested NP appears as red fluorescent dots and is located within the cytoplasm of green $CD68^{+}$ BMM. BMM-released IDV was assayed by RP-HPLC from cell lysates was performed (B). With subsequent media changes (wash, arrowheads) extracellular (media) and intracellular (BMM) IDV levels diminished (C).

NIH-PA Author Manuscript
NIH-PA Author Manuscript
NIH-PA Author Manuscript

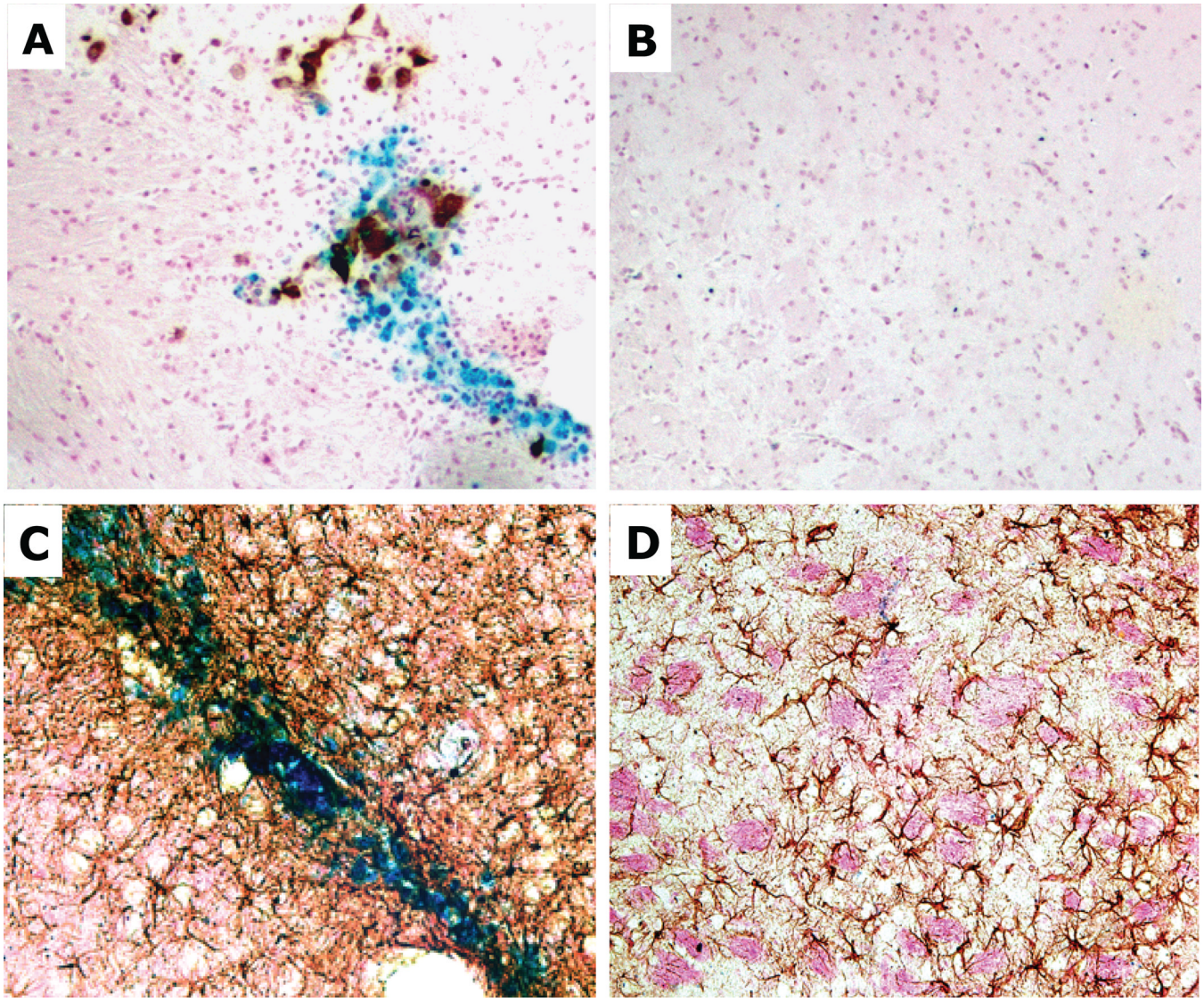

FIGURE 2.

BMM migration to HIVE affected brain tissue. SPIO-BMM were injected intravenously into HIVE or sham-operated mice. Histology assay examined BMM migration to diseased brain sites. Sections of brain from HIVE (A, C) and sham (B and D) mice were immunostained for HIV-1 p24 (A and B, brown) and GFAP for astrocytes (C and D, brown). Prussian blue staining (blue) revealed SPIO-labeled BMM (A and C, blue) migration into the area of HIV-1 infected MDM 5 days after adoptive transfer of BMM to recipient mice. In sham-operated mice (B and D), no significant BMM migration was detected. Original magnifications, × 200.

NIH-PA Author Manuscript
NIH-PA Author Manuscript
NIH-PA Author Manuscript

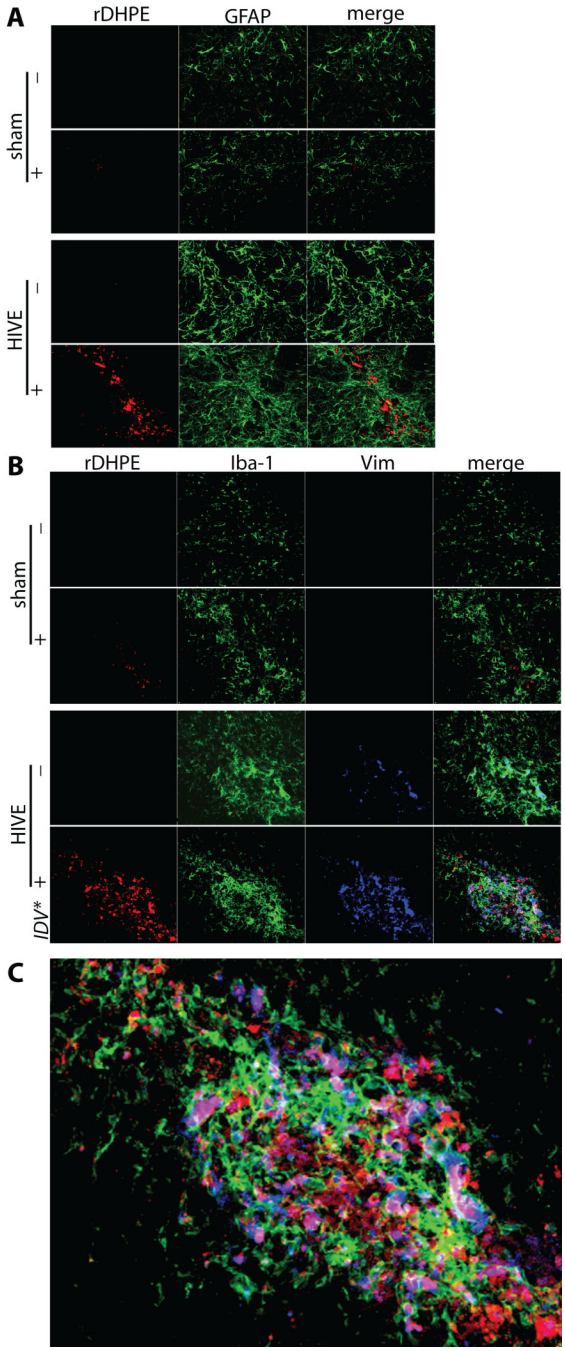

FIGURE 3.

Neuroinflammatory responses affect BMM migration. Stereotactic injection of HIV-1 infected MDM into the caudate/putamen of SCID mice was used to induce HIVE resulting in neuroinflammation by astrocytes and microglia activation. Immunostaining was performed on frozen brain sections from sham-operated and HIVE mice with or without rDHPE-IDV-NP-BMM. Confocal imaging of Iba-1 (green, A) and GFAP (green, B) immunoreactivity reflects astrogliosis and microgliosis responses. The red fluorescence spots were around and within the site of injection in HIVE mice 3 days after rDHPE-IDV-NP-BMM treatment. rDHPE-IDV-NP-BMM are co-located with GFAP reactive astrocytes in HIVE mice when compared to sham-operated animals (A). Confocal imaging of Iba-1 (green) reflects microgliosis (B). The

NIH-PA Author Manuscript

NIH-PA Author Manuscript

NIH-PA Author Manuscript

Vim (blue) staining was used to distinguish between the human MDM and murine microglia in B with composite of IDV, Vim and Iba-1 immunostaining in C. The red rDHPE-IDV-NP-BMM differentiated microglia from migrated BMM. However, Iba-1 also labeled native circulating monocytes in the mice. Moreover, sham mice showed minimal glial reactions as visualized by GFAP and Iba-1 (green) in response to needle trauma with few rDHPE-IDV-NP-BMM. The photomicrograph shows BMM migration and brain immune responses in the infected animals. IDV* denotes rDHPE-IDV-NP-BMM. Original magnification, × 200.

NIH-PA Author Manuscript
NIH-PA Author Manuscript
NIH-PA Author Manuscript

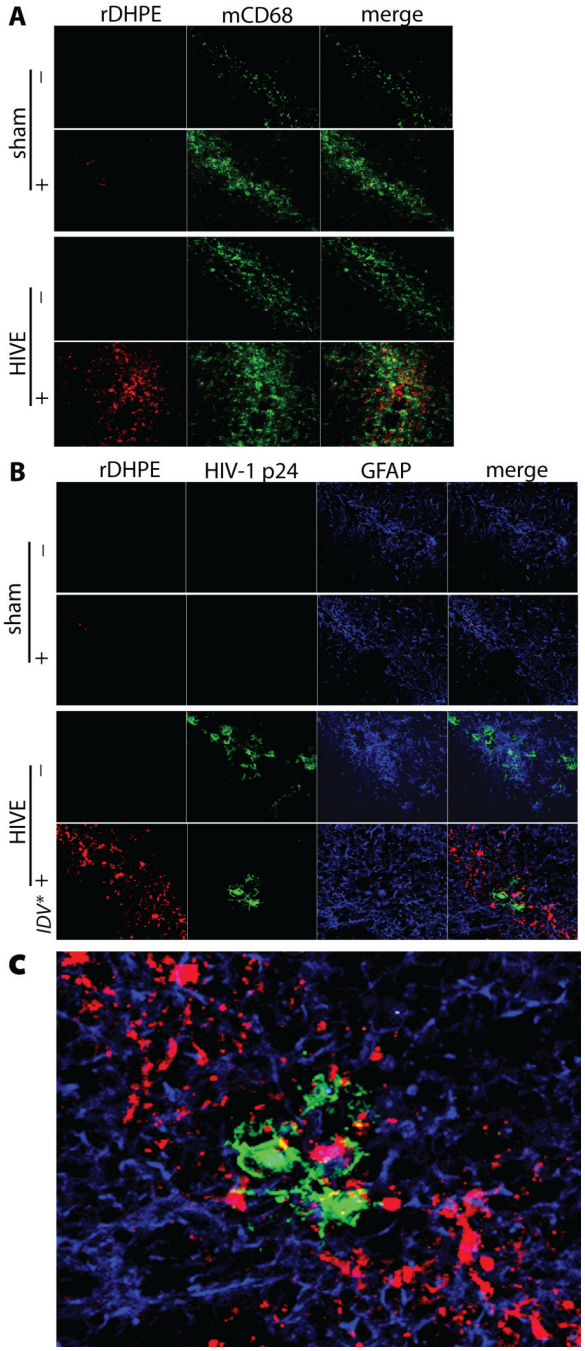

FIGURE 4.

Brain tissue distributions of rDHPE-IDV-NP-BMM. Sham and HIVE mice were injected with rDHPE-IDV-NP-BMM for 3 days, and frozen brain sections were stained with antibody to CD68, HIV-1p24 and GFAP (A and B). Confocal microscopy was used to assess the distribution of $CD68^+$ cells (green) in and around injection areas of the brain in both sham and HIVE animals 3 days after IDV-NP-BMM treatment. $CD68^+$ cells were located in and surrounding the injection line in all animals seen in A. The intensity of $CD68^+$ cells was associated with rDHPE-IDV-NP-BMM (red, A) in treated mice compared to untreated mice in all groups. A substantial increase of rDHPE-IDV-NP-BMM (red, B) was observed in viral infection areas in HIVE mice compared to sham and MDM animals. Confocal imaging of brain

NIH-PA Author Manuscript

NIH-PA Author Manuscript

NIH-PA Author Manuscript

sections with double immunostaining to HIV-1p24 (green, B) and GFAP (blue, B) showed increased red fluorescence (rDHPE-IDV-NP-BMM) in brain areas where there was active viral infection (HIV-1p24^{+} MDM). Greater levels of rDHPE-IDV-NP-BMM were in HIVE compared to sham animals. GFAP (blue, B) and rDHPE-IDV-NP-BMM (red, B) were linked to HIV-1 infection and GFAP astrogliosis (green, B and C); however, there was no correlation between rDHPE-IDV-NP-BMM levels and GFAP expression in treated animals compared to untreated mice in sham and HIVE mouse groups. IDV* denotes rDHPE-IDV-NP-BMM. Original magnification, × 200.

NIH-PA Author Manuscript
NIH-PA Author Manuscript
NIH-PA Author Manuscript

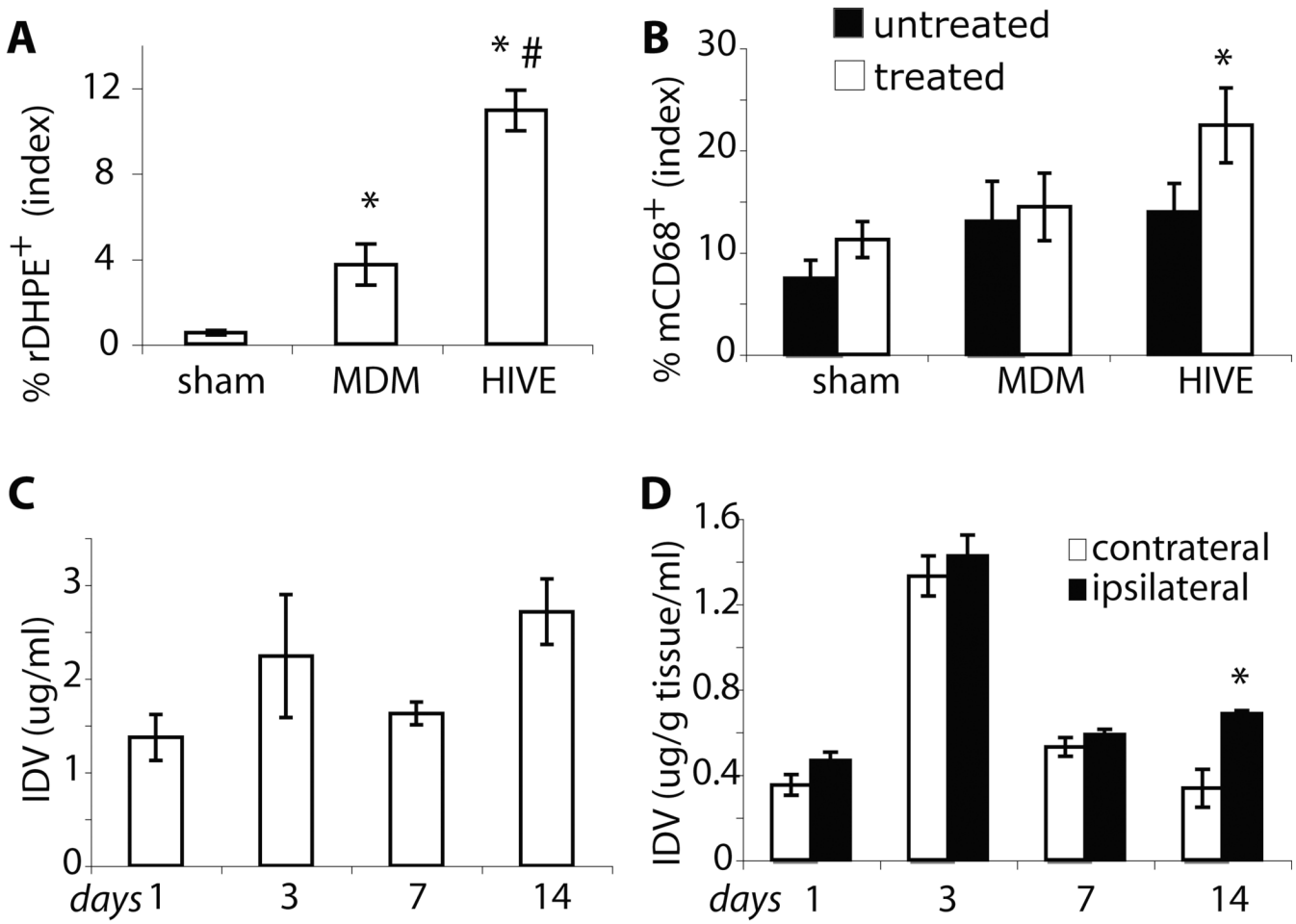

FIGURE 5.

Brain tissue IDV concentration. Quantitative image analysis assayed the distribution of rDHPE-IDV-NP-BMM and $CD68^+$ cells (A). The levels of rDHPE-IDV-NP-BMM (open bar) were significantly increased in HIVE compared to both sham-operated and MDM mice. Untreated animals counted as 0 (black bar). *$p < 0.05$ compared to sham and #$p < 0.05$ compared to MDM. $CD68^+$ cells were assayed in the same brain slides by quantitative image analysis of untreated (closed bar) or treated (open bar) with rDHPE-IDV-NP-BMM (B). Mean (± SEM) percent area distribution of rDHPE-IDV-NP-BMM was determined for 5 mice per group. * $p < 0.05$ compared to untreated. IDV levels were assayed by HPLC from blood in HIVE mice treated with IDV-NP-BMM at day 1, 3, 7 and 14 (C and D). With a single dosage of treatment, IDV levels were testable by HPLC until reaching day 14. Blood IDV levels were obtained in treated HIVE mice at experimental time points after i.v injection via the tail vein. Mean (± SEM) μg of IDV/ ml blood was determined for 5 mice per group. IDV were assayed by HPLC from lysates of brain tissues (D). The diseased (ipsilateral) brain tissue levels of IDV were analyzed and compared to the contralateral hemisphere at the experimental time points. Mean (± SEM) μg of IDV/100mg brain tissue was determined for 5 mice per group. *$p < 0.01$ compared to the contralateral hemisphere.

NIH-PA Author Manuscript

NIH-PA Author Manuscript

NIH-PA Author Manuscript

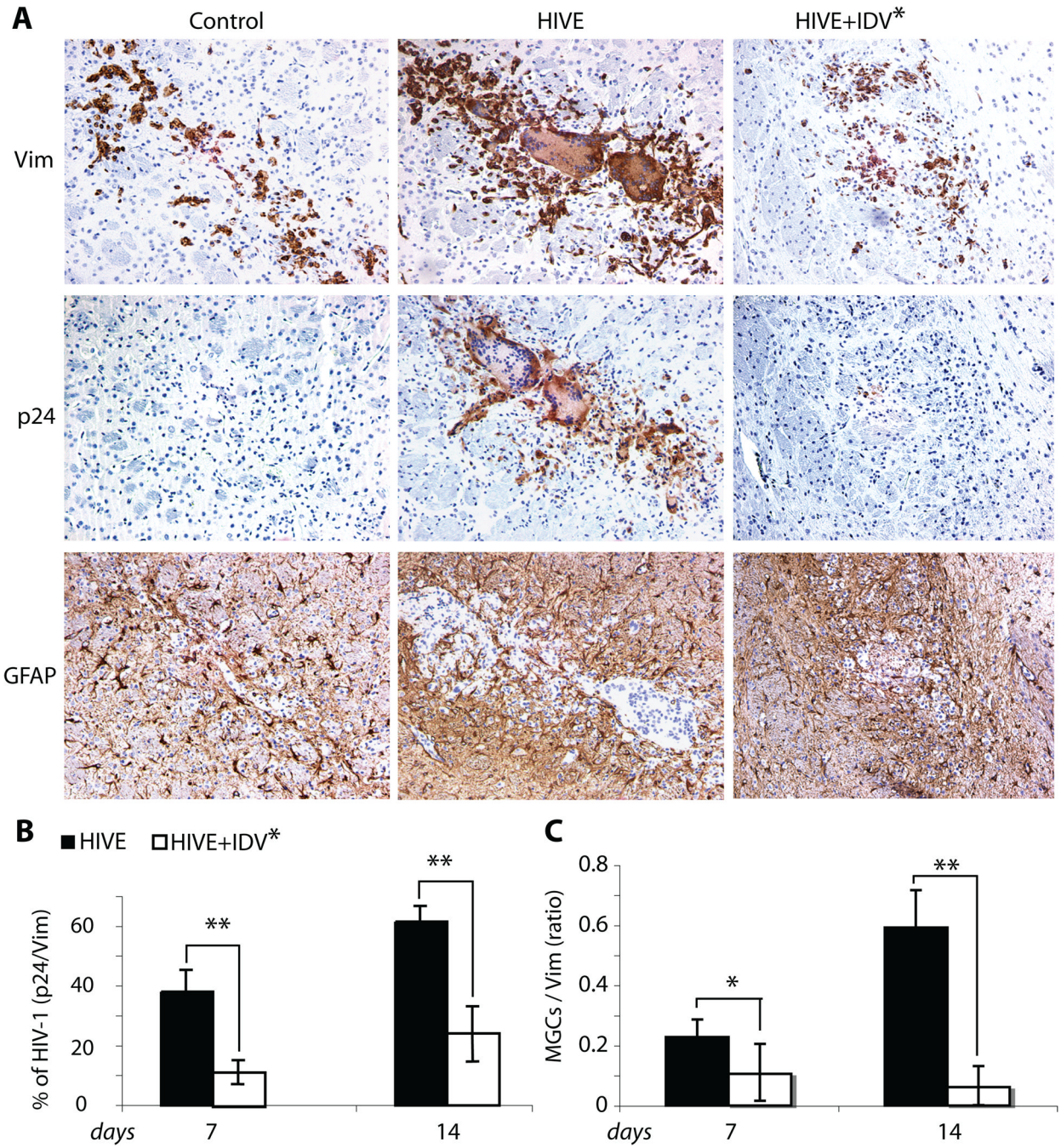

FIGURE 6.

Antiretroviral activities of IDV-NP-BMM in HIVE mice. Stereotactic injection of HIV-1 infected MDM into the caudate/putamen of SCID mice was utilized to induce HIVE with resulting neuroinflammation, viral infection and neuronal injury. Immunostaining was performed on paraffin brain sections from HIVE mice (those animals injected with virus-infected MDM) with or without IDV-NP-BMM treatment (designated as HIVE and HIVE and IDV, respectively). Staining for Vim, HIV-1p24, and GFAP (brown) reflect the presence of human MDM, virus-infected cells, and neuroinflammatory responses (A). Microscopic images of human Vim^+ and HIV-1 $p24^+$ MDM and $GFAP^+$ astrocytes showing similar human MDM reconstitution and astrogliosis were observed in the brains of all groups. Original

NIH-PA Author Manuscript

NIH-PA Author Manuscript

NIH-PA Author Manuscript

magnification, × 200. Numbers of virus-infected MDM were assayed by percentage of HIV-1 $p24^+/Vim^+$ stained cells (B). A significant decrease in numbers of virus-infected cells was observed in IDV-NP-BMM treated HIVE mice. MGC, a known pathological hallmark of HIVE, were found in injection sites where HIV-1 $p24^+$ were seen (A and C). Reduced numbers of MGC, and with reduced size, were seen in antiretroviral-treated HIVE mice. MGC formation was determined by numbers of MGC/total number of Vim^+ MDM (Mean ± SEM) (C). IDV* represents IDV-NP-BMM. *$p < 0.01$ and **$p < 0.01$ compared to untreated HIVE mice.

NIH-PA Author Manuscript

NIH-PA Author Manuscript

NIH-PA Author Manuscript

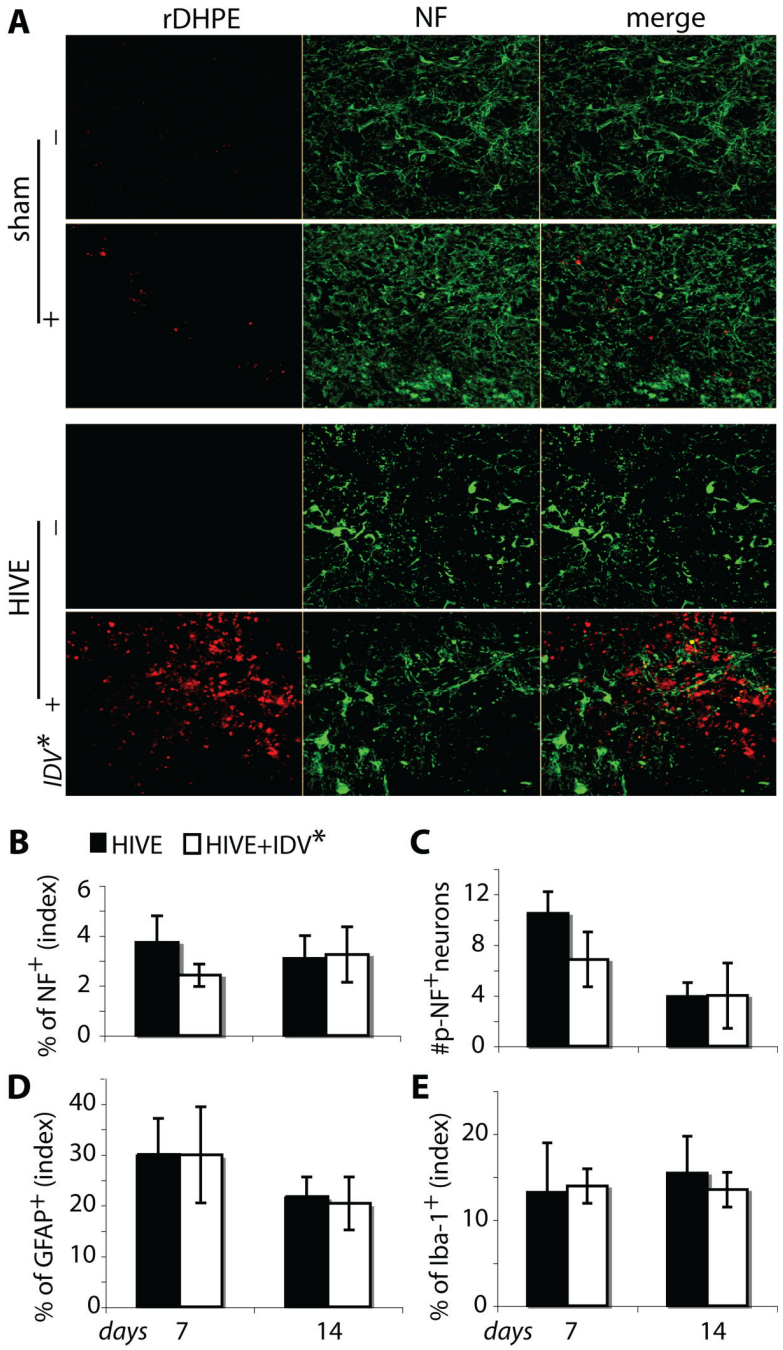

FIGURE 7.

IDV-NP-BMM does not affect neural morphology. Neuronal immunostaining for NF, which included both the NF and p-NF forms, was performed in brain tissue sections of SCID mice 3 days after a single intravenous injection of rDHPE-IDV-NP-BMM (A). SCID mice were intracranially injected with saline, MDM or HIV-1 infected MDM. Serial 25 μm frozen brain tissue sections were stained with antibodies to NF (green). Spatial relationships between NF^+ axon loss and p-NF neuronal body accumulation in viral infection were determined by confocal image analysis. The local rDHPE-IDV-NP-BMM (red) distribution showed no changes in NF^+ axon loss and p-NF accumulation compared to three groups of animals that did not receive treatment. Original magnification, 200 X. Quantitative image analyses was used

NIH-PA Author Manuscript

NIH-PA Author Manuscript

NIH-PA Author Manuscript

to assess immunostaining of NF (B), p-NF (C), GFAP (D) and Iba-1 (E). Absolute number of p-NF^+ neuronal bodies was counted in HIVE mice with or without IDV-NP-BMM treatment. These results showed that there was no relationship between IDV-NP-BMM levels to either neuronal injury or neuroinflammatory responses. IDV* represents rDHPE-IDV-NP-BMM.

NIH-PA Author Manuscript

NIH-PA Author Manuscript

NIH-PA Author Manuscript

Table 1

Antiretroviral activities of IDV-NP-BMM

Days	**7**		**14**	
Antibodies	**Vim+**	**HIV-1p24+**	**Vim+**	**HIV-1p24+**
MDM	368.88 ± 43.54	0	93.5 ±12.24	0
HIVE	419.11 ± 45.64	128.5 ± 31.35	103.17 ± 12.53	62 ± 5.02
HIVE and BMM-IDV-NP	342.26 ± 18.88	52.67 ± 20.12*	81.63 ± 19	22.88 ± 9.86*

Absolute numbers of Vim^+ and HIV-1 $p24^+$ MDM were determined from serial immunohistological sections. These were used to assess levels of HIV-1 infection. Mean (± SEM) are absolute numbers of Vim^+ and HIV-1 $p24^+$ MDM determined for 5 animals per group. IDV-NP-BMM intravenous administration significantly reduced levels of HIV-$1p24^+$ MDM when compared to untreated HIVE mice. Uninfected MDM injected into the subcortex of immunodeficient mice served as a control.

* $p < 0.05$ compared IDV-NP-BMM treated to untreated HIVE mice.